Journal of the Arkansas Academy of Science

Volume 60 Article 10

2006

Electron Shock Waves

Mostafa Hemmati
Arkansas Tech University, mhemmati@atu.edu

Michael Weller
Arkansas Tech University

Taylor Duncan
Arkansas Tech University

Follow this and additional works at: https://scholarworks.uark.edu/jaas

 Part of the Physical Chemistry Commons

Recommended Citation

Hemmati, Mostafa; Weller, Michael; and Duncan, Taylor (2006) "Electron Shock Waves," *Journal of the Arkansas Academy of Science*: Vol. 60, Article 10.
Available at: https://scholarworks.uark.edu/jaas/vol60/iss1/10

This article is available for use under the Creative Commons license: Attribution-NoDerivatives 4.0 International (CC BY-ND 4.0). Users are able to read, download, copy, print, distribute, search, link to the full texts of these articles, or use them for any other lawful purpose, without asking prior permission from the publisher or the author.
This Article is brought to you for free and open access by ScholarWorks@UARK. It has been accepted for inclusion in Journal of the Arkansas Academy of Science by an authorized editor of ScholarWorks@UARK. For more information, please contact scholar@uark.edu, uarepos@uark.edu.

Electron Shock Waves

MOSTAFA HEMMATI[1,2], MICHAEL WELLER[1], AND TAYLOR DUNCAN[1]

[1]*Department of Physical Science, Arkansas Tech University, Russellville, AR 72801*

[2]Correspondence: mhwmmati@atu.edu

Abstract.—In this paper we describe numerical investigations of breakdown waves concentrating on antiforce waves. We employed one-dimensional electron fluid dynamical equations for a luminous pulse wave propagating into a neutral gas region and subjected to an applied electric field. We assumed that the electrons were the main element in the propagation of the wave and that the electron gas partial pressure provided the driving force. These waves are considered to be shock fronted and are composed of two regions: the thin sheath region behind the shock front and the thicker quasi-neutral region following the sheath region. Our set of equations, known as the electron fluid dynamical (EFD) equations, is composed of the equations of conservation of mass, momentum, and energy coupled with Poisson's equation. For antiforce waves, we were able to successfully integrate the set of EFD equations through the sheath region using a set of initial boundary conditions at the wave front. By using values of electron gas temperature, electron number density, ionization rate, and also the existing conditions at the end of the sheath region as initial boundary values for the thermal region of the gas, we were able to integrate the electron fluid dynamical equations, modified for the thermal region of the gas, through that region. Our results satisfy the required conditions at the end of the sheath and quasi-neutral regions. The wave profiles for electric field, electron velocity, electron number density, electron gas temperature, and ionization rate within the sheath and quasi-neutral regions were determined.

Key words.—Breakdown waves, one-dimensional electron fluid dynamical (EFD) equations, luminous pulse wave, electrons.

Introduction

Lightning has always been an awe-inspiring event that has intrigued and perplexed men since the beginning of history. This is the pinnacle example of luminous fronts, or pulses, generated by potential differences between two points in a gas. Von Zahn (1879) proposed lack of Doppler shift in the radiation emitted from breakdown waves, inferring negligible mass motion within the pulse. Thomson (1893) made the observation that breakdown waves moved at approximately half the speed of light, rather than instantaneously jumping from one point to another.

Beams (1930) then proved Thomson's observations correct and proposed an explanation for this phenomenon: that the gas behind the pulse was electrically conductive, thereby carrying a potential and creating a breakdown of the gas in the given area as the wave propagates. He also explained that because of the large mass difference between the positive ions and the electrons, the positive ions, as compared to the electrons, will have a negligible increase in speed. This explanation is still accepted today. Paxton and Fowler (1962) applied a three-fluid, hydrodynamical model to formulate a set of equations describing the wave propagation.

Shelton and Fowler (1968) continued this work and described the phenomena as "electron fluid dynamical" waves. They developed a set of one-dimensional equations describing the phenomena, deriving equations for energy and momentum loss and gain terms during the electron collisions with heavy particles. Their main concern was proforce waves, waves for which the electric field force on electrons is in the same direction as the direction of the propagation of the pulse. We will concentrate on antiforce waves, waves for which the electric field force on electrons is in the opposite direction of the propagation of the wave. Using an approximation method, Fowler and Shelton (1973) solved their set of electron fluid dynamical equations for the dynamical transition region of the wave. Their approximate solutions are in good agreement with experimental data available (Blais and Fowler 1973).

Later, Sanmann and Fowler (1975) tried to account for the propagation of antiforce waves. They considered the electron gas partial pressure to be much larger than that of the other species, therefore providing the driving force for the propagation of the wave. Fowler et al. (1984) completed the set of electron fluid dynamical equations by adding terms to the equation of conservation of energy, which proved to be essential for exact numerical solution of the set of electron fluid dynamical equations. They also developed a computer program to integrate the equations through the sheath region. Hemmati (1999) completed the set of electron fluid dynamical equations representing the antiforce waves. Rakov (2000) provided a complete set of experimental results for the wave speed, current, and charge in his review of positive and bipolar lightning discharges.

Analysis

The equations which were fully developed by Fowler et al. (1984), representing a one-dimensional, steady state, constant velocity, electron fluid dynamical wave propagating into a neutral medium, are the equations of conservation of mass, momentum, and energy coupled with Poisson's equation:

$$\frac{d(nv)}{dx} = n\beta, \quad [1]$$

$$\frac{d}{dx}[mnv(v-V) + nkT_e] = -enE - Kmn(v-V), \quad [2]$$

$$\frac{d}{dx}[mnv(v-V)^2 + nkT_e(5v-2V) + 2envΦ - \frac{5nk^2T_e}{mK}\frac{dT_e}{dx}] = -3(\frac{m}{M})nkKT_e - (\frac{m}{M})Kmn(v-V)^2, \quad [3]$$

$$\frac{dE}{dx} = \frac{e}{\varepsilon_0}n(\frac{v}{V} - 1); \quad [4]$$

where n, v, T_e, e, and m are the electron number density, velocity, temperature, charge, and mass, respectively. M, E, E_o, V, k, K, x, β, and φ are neutral particle mass, electric field within the sheath region, electric field at the wave front, wave velocity, Boltzmann's constant, elastic collision frequency, position within the sheath region, ionization frequency, and ionization potential of the gas, respectively.

To reduce the set of electron fluid dynamical equations to non-dimensional form, the following set of dimensionless variables are introduced:

$$\eta = \frac{E}{E_o}, \nu = (\frac{2e\phi}{\varepsilon_o E_o^2})n, \psi = \frac{v}{V}, \theta = \frac{T_e k}{2e\phi}, \xi = \frac{eE_o x}{mV^2},$$
$$\alpha = \frac{2e\phi}{mV^2}, \kappa = \frac{mV}{eE_o}K, \mu = \frac{\beta}{K}, \omega = \frac{2m}{M},$$

where η, ν, ψ, θ, μ, and ξ represent the dimensionless net electric field (applied plus space charge field), electron number density, electron velocity, electron gas temperature, ionization rate, and position within the sheath region, respectively. α and κ are wave parameters.

Substituting the dimensionless variables in equations (1-4) reduces them to the following form:

$$\frac{d(\nu\psi)}{d\xi} = \kappa\mu\nu, \quad [5]$$

$$\frac{d}{d\xi}[\nu\psi(\psi-1) + \alpha\nu\theta] = -\nu\eta - \kappa\nu(\psi-1), \quad [6]$$

$$\frac{d}{d\xi}[\nu\psi(\psi-1)^2 + \alpha\nu\theta(5\psi-2) + \alpha\nu\psi + \alpha\eta^2 - \frac{5\alpha^2\nu\theta}{\kappa}\frac{d\theta}{d\xi}] = -\omega\kappa\nu[3\alpha\theta + (\psi-1)^2], \quad [7]$$

$$\frac{d\eta}{d\xi} = \frac{\nu}{\alpha}(\psi - 1). \quad [8]$$

Shelton and Fowler (1968) proposed the existence of two distinct regions within the wave: the sheath and the quasi-neutral region. In the sheath region, electron velocity, starting from an initial value at the shock front, reduces to speeds comparable to those of heavy particles. Also, the electric field, starting with its maximum value at the shock front, reduces to a negligible value at the trailing edge of the sheath. These conditions translate into the following equation form:

$$\psi_2 = 1, \eta_2 = 0, \psi_2' = 0, \text{ and } \eta_2' = 0, \quad [9]$$

where, ψ_2, η_2, ψ_2', and η_2' are the non-dimensional electron velocity, electric field, electron velocity derivative, and electric field derivative at the end of the sheath region, respectively.

In the quasi-neutral region, through further ionization of neutral particles, the electron gas cools to near room temperatures. Therefore, the electric field energy present ahead of the wave is converted to ionization energy behind the wave. In non-dimensional form the expected conditions at the end of the quasi-neutral region are as follows:

$$\nu_f = 1 \text{ and } \theta_f = 0.065.$$

All of our attempts at integrating equations 5-8 through the quasi-neutral region failed. Equations 5-8 were derived by combining the primitive forms of the fluid equations, and since we were not using approximation methods for solving the set of fluid equations, there was no need for the combined form of the equations. Therefore, for our investigation of the quasi-neutral region of the wave, we chose the primitive form of the electron-fluid dynamical equations:

$$\frac{d(\nu\psi)}{d\xi} = \kappa\mu\nu, \quad [10]$$

$$\frac{d}{d\xi}[\nu\psi^2 + \alpha\nu\theta] = -\nu\eta - \kappa\nu(\psi-1) + \kappa\mu\nu, \quad [11]$$

$$\frac{d}{d\xi}(v\psi^3 + 5v\psi\alpha\theta - \frac{5\alpha^2 v\theta}{\kappa}\frac{d\theta}{d\xi}) =$$
$$-2v\psi\eta - 2\kappa v(\psi - 1) + \kappa\mu v(\psi - 1) - \omega\kappa v[3\alpha\theta + (\psi - 1)^2], \quad [12]$$

$$\frac{d\eta}{d\xi} = \frac{v}{\alpha}(\psi - 1). \quad [13]$$

By applying the expected conditions at the end of the sheath region [9] in the expanded forms of the equations of conservation of mass and momentum [10-11], the equations describing the quasi-neutral region become

$$v_2^{'} = \kappa\mu_2 v_2 \quad [14]$$

and

$$\theta_2^{'} = -\kappa\mu_2\theta_2 \quad [15]$$

where v′2 and θ′ 2 are the electron number density derivative and electron gas temperature derivative in the quasi-neutral region.

By integrating equations 5-8 through the sheath region, one can find the electron number density, electron gas temperature, and ionization rate values at the end of the sheath region. These variables now become the initial boundary conditions for the quasi-neutral region. We have been able to successfully integrate equations 14-15 through the quasi-neutral region of the wave and our results meet the expected conditions at the trailing edge of the wave ($v_f = 1$ and $\theta_f = 0.065$).

For antiforce waves, slight changes in the electron fluid dynamical equations need to be made. For an observer stationary relative to the wave front, the heavy particles move in the negative x direction ($V < 0$, $E_o > 0$, and $K > 0$). Therefore, both κ and ξ will be intrinsically negative. For antiforce waves, therefore, the set of dimensionless variables is slightly different and has been derived by Hemmati (1999):

$$\eta = \frac{E}{E_o}, v = (\frac{2e\phi}{\varepsilon_o E_o^2})n, \psi = \frac{v}{V}, \theta = \frac{T_e k}{2e\phi}, \xi = -\frac{eE_o x}{mV^2},$$
$$\alpha = \frac{2e\phi}{mV^2}, \kappa = -\frac{mV}{eE_o}K, \mu = \frac{\beta}{K}, \omega = \frac{2m}{M}.$$

The equations describing antiforce waves in non-dimensional form are therefore

$$\frac{d}{d\xi}[v\psi] = \kappa\mu v, \quad [16]$$

$$\frac{d}{d\xi}[v\psi(\psi - 1) + \alpha v\theta] = v\eta - \kappa v(\psi - 1), \quad [17]$$

$$\frac{d}{d\xi}[v\psi(\psi - 1)^2 + \alpha v\theta(5\psi - 2) + \alpha v\psi + \alpha\eta^2 - \frac{5\alpha^2 v\theta}{\kappa}\frac{d\theta}{d\xi}] =$$
$$-\omega\kappa v[3\alpha\theta + (\psi - 1)^2], \quad [18]$$

$$\frac{d\eta}{d\xi} = -\frac{v}{\alpha}(\psi - 1). \quad [19]$$

Results

The electron velocity at the wave front is less than the wave velocity ($v_1 < V$). The dimensionless electron velocity at the wave front, ψ_1, therefore must be less than 1. As a result, according to the Poisson's equation, the electric field will have a positive slope behind the wave front resulting in an initial increase in the electric field. Heading through the sheath region following the shock front, the electric field will increase until the electrons gain speed in excess of ion speeds. The dimensionless electron velocity will then become larger than 1, making the electric field slope negative. The electric field therefore decreases (Hemmati 1995) until the electrons slow down to speeds comparable to ion speeds at the end of the sheath region ($\psi_2 \rightarrow 1$), requiring that the electric field and its slope approach zero at the end of the sheath as well ($\eta_2 \rightarrow 0, \eta_2^{'} \rightarrow 0$).

We used a trial and error method to integrate equations 16-19. For a given wave speed, α, we chose a set of values for wave constant, κ, electron velocity, ψ_1, and electron number density, v_1, at the shock front. We repeatedly changed the values of κ, ψ_1, and v_1, in the process of integration of equations 16-19 so that the process led to a conclusion in agreement with the expected conditions [9] at the end of the sheath region. As in the proforce case, we used the conditions at the end of the sheath region to find the equations describing the quasi-neutral region. For integrating the set of equations describing the quasi-neutral region, we used electron temperature, electron number density, and ionization rate values at the end of the sheath region as initial boundary values for the quasi-neutral region. For antiforce waves, we were successful in integrating the electron-fluid dynamical equations through both the sheath and quasi-neutral regions for two values of wave speeds, $\alpha = 0.05$ and $\alpha = 1$, representing wave velocities of 1.33×10^7 m/s and 2.96×10^6 m/s, respectively. For $\alpha = 0.05$, the initial boundary conditions required were $\kappa = 0.35$, $\psi_1 = 0.95$, and $v_1 = 0.09$. For $\alpha = 1$, the conditions required at the shock front were $\kappa = 0.17$, $\psi_1 = 0.98$, and $v_1 = 0.40$.

Figure 1 represents electric field, η, as a function of position, ξ, inside the sheath region. As it can be seen, the electric field approaches zero as it nears the end of the sheath. For α =

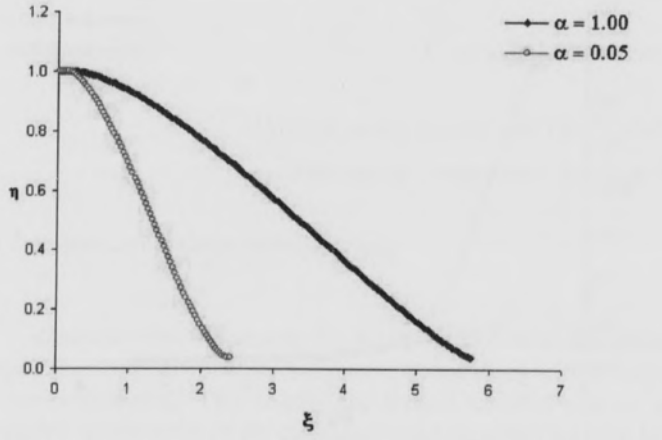

Fig. 1. Electric field, η, as a function of position, ξ, inside the sheath region for $\alpha = 0.05$ and $\alpha = 1$.

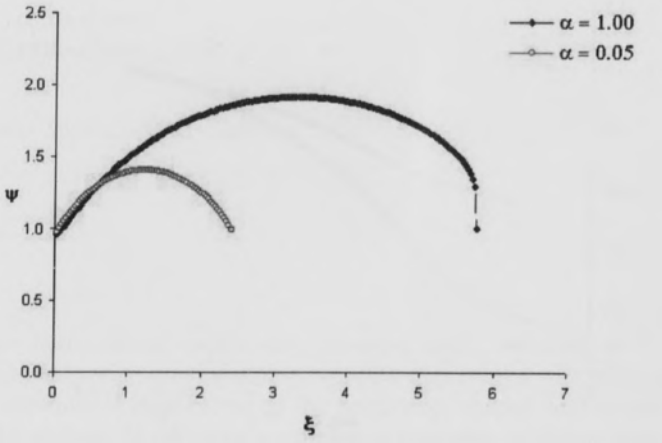

Fig. 2. Electron velocity, ψ, as a function of position, ξ, inside the sheath region for $\alpha = 0.05$ and $\alpha = 1$.

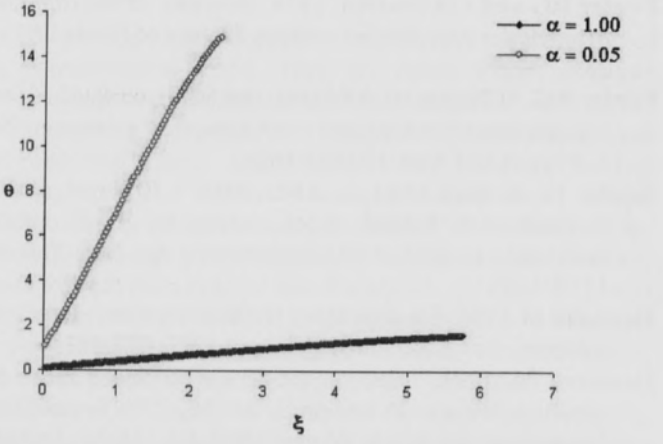

Fig. 3. Electron temperature, θ, as a function of position, ξ, inside the sheath region for $\alpha = 0.05$ and $\alpha = 1$.

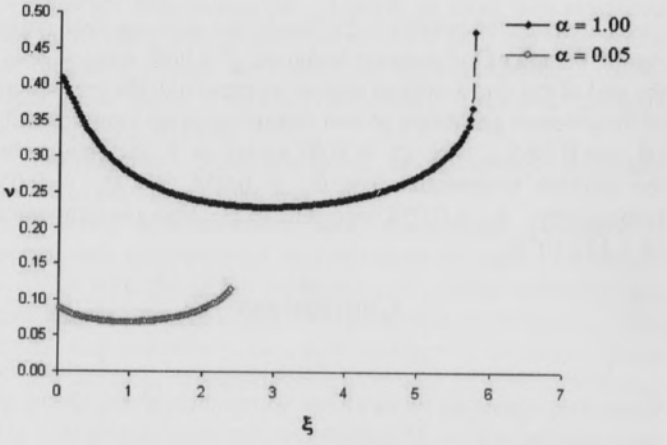

Fig. 4. Electron number density, ν, as a function of position, ξ, inside the sheath region for $\alpha = 0.05$ and $\alpha = 1$.

0.05 and $\alpha = 1$, the sheath region goes to $\xi = 2.41$ and $\xi = 5.75$, respectively; representing sheath thicknesses of 2.43×10^{-6} m and 2.87×10^{-5} m, respectively. Figure 2 represents electron velocity, ψ, as a function of position, ξ, inside the sheath region. As expected, the dimensionless velocity goes to one as it approaches the end of the sheath region.

Figure 3 represents electron temperature, θ, as a function of position, ξ, inside the sheath region. For $\alpha = 0.05$ and $\alpha = 1$, the electron temperature goes to $\theta = 14.868$ and $\theta = 1.623$, respectively at the end of the sheath region. $\theta = 14.868$ and $\theta = 1.623$ represent electron gas temperatures of 8.62×10^{6} K and 9.41×10^{5} K, respectively. Figure 4 represents electron number density, ν, as a function of position, ξ, inside the sheath region. For $\alpha = 0.05$ and $\alpha = 1$, the electron number density goes to $\nu = 0.1145$ and $\nu = 0.4726$, respectively at the end of the sheath region. $\nu = 0.1145$ and $\nu = 0.4726$ represent electron number densities of 1.26×10^{19} /m^3 and 5.21×10^{19} /m^3, respectively.

Figure 5 represents electron number density, ν, as a function of position, ξ, inside the quasi-neutral region. The log of position is graphed for simplification. As expected, the dimensionless electron number density approaches one ($\nu_f \rightarrow 1$) for both wave speeds at the end of the quasi-neutral region. $\nu_f = 1.0$ represents an electron number density of 1.10×10^{20} /m^3. Figure 6 represents electron temperature, θ

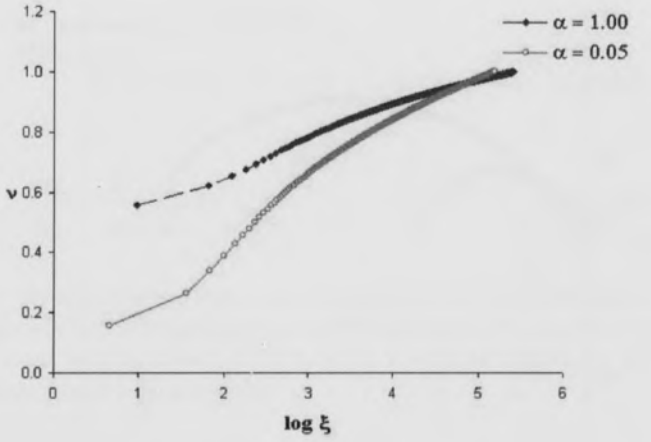

Fig. 5. Electron number density, ν, as a function of position, ξ, inside the QNR for $\alpha = 0.05$ and $\alpha = 1$.

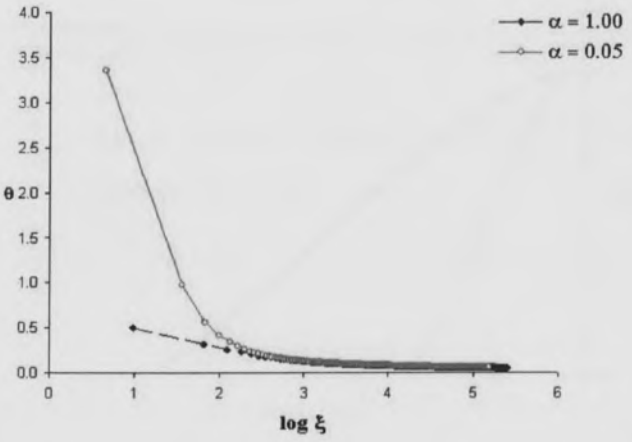

Fig. 6. Electron temperature, θ, as a function of position, ξ, inside the QNR for $\alpha = 0.05$ and $\alpha = 1$.

, as a function of position, ξ, inside the quasi-neutral region. Again, the log of the position is shown. For both wave speeds at the end of the quasi-neutral region, as expected, the temperature of the electron gas drops so that ionization is no longer possible ($\theta_f \rightarrow 0.065$). For $\alpha = 0.05$ and $\alpha = 1$, the final values for electron temperature are $\theta_f = 0.054$ and $\theta_f = 0.052$, respectively. $\theta_f = 0.054$ represent an electron gas temperature of 3.13×10^4 K.

Conclusions

In our research we successfully integrated the electron fluid dynamical equations for antiforce waves through the sheath and quasi-neutral region. The results for the wave speeds $\alpha = 0.05$ and $\alpha = 1$ conform to the expected conditions at the end of both the sheath and quasi-neutral region. Our selected wave speeds and calculated electron number densities and electron gas temperatures compare well with the observations of Uman et al. (1968), Rakov (2000), and Fujita et al. (2003). This is yet another confirmation of the validity of the fluid model used to describe breakdown waves.

ACKNOWLEDGMENTS.—The authors would like to express their gratitude to the Arkansas Space Grant Consortium for their continued financial support of this research.

Literature Cited

Beams J W. 1930. The propagation of luminosity in discharge tubes. Physical Review 36:997-1002.

Blais RN and RG Fowler. 1973. Electron wave breakdown of helium. Physics of Fluids 16(12):2149-2154.

Fowler RG and GA Shelton. 1974. Structure of electron fluid dynamical waves: Proforce waves. Physics of Fluids 17:334-339.

Fowler RG, M Hemmati, RP Scott, and S Parsenajadh. 1984. Electric breakdown waves: exact numerical solutions. Part I. Physics of Fluids 27:1521-1526.

Fugita K, S Sato, and T Abe. 2003. Electron density measurements behind shock waves by H-β profile matching. Journal of Thermodynamics and Heat Transfer 17:210-216.

Hemmati M. 1995. Electron shock waves moving into an ionized medium. Laser and Particle Beams. 13(3):377-382.

Hemmati M. 1999. Electron shock waves: Speed range for antiforce waves. Proceedings of the 22nd International Symposium on Shock Waves; 1999 July 18-23; Imperial College, London, UK. Imperial College 2:995-1000.

Paxton GW and RG Fowler. 1962. Theory of breakdown wave propagation. Physical Review 128: 933-9977.

Rakov VA. 2000. Positive and bipolar lightning discharges: A review. Proceedings of the 25th International Conference on Lightning Protection; 2000 September 18-22; Rhodes, Greece. 103-108.

Sanmann E and RG Fowler. 1975. Structure of electron fluid dynamical plane waves: Antiforce waves. The Physics of Fluids 18:1433-1438.

Shelton GA and RG Fowler. 1968. Nature of electron fluid dynamical waves. The Physics of Fluids 11(4):740-746.

Thomson JJ. 1893. Recent Researchers. New York, Oxford University Press, p. 115.

Uman MA, RE Orville, and **AM Sletten.** 1968. Four-meter sparks in air. Journal of Applied Physics 39:5162-5168.

Von Zahn W. 1879. Edited by G. Wiedemann. Spectralrohren mit longitudinaler Durch- sicht. Annalen der. physic. 1-47:675-678.